analytical chemistry

pubs.acs.org/ac Letter

Facile Determination of Phosphorylation Sites in Peptides Using Two-Dimensional Mass Spectrometry

Johanna Paris, Tomos E. Morgan, Christopher A. Wootton, Mark P. Barrow, John O'Hara, and Peter B. O'Connor*

Cite This: *Anal. Chem.* 2020, 92, 6817−6821 Read Online

ACCESS | Metrics & More | Article Recommendations | Supporting Information

ABSTRACT: Detection and characterization of phosphopeptides by infrared multiphoton dissociation two-dimensional mass spectrometry (IRMPD 2DMS) is shown to be particularly effective. A mixture of phosphopeptides was analyzed by 2DMS without any prior separation. 2DMS enables the data independent analysis of the mixture and the correlation of the fragments to their precursor ions. The extraction of neutral loss lines corresponding to the loss of phosphate under IRMPD fragmentation allows the selective identification of phosphopeptides. Resonance of the 10.6 μm infrared radiation with the vibrational modes of the phosphate functional group produced efficient absorption and high cleavage coverage of the phosphopeptides at much lower irradiation fluence than for nonphosphorylated peptides improving discrimination. Additionally, the localization of the phosphate group was determined.

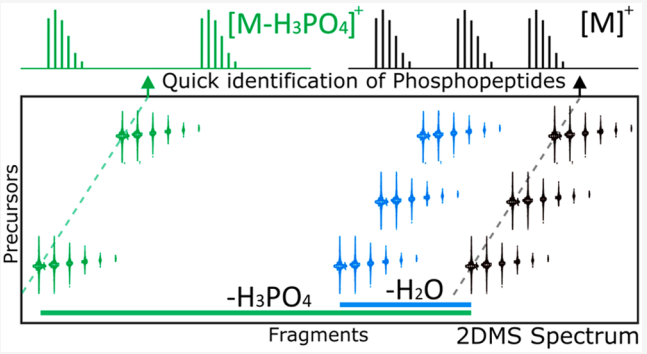

Thousands of proteins are expressed in mammalian cells; a third of them are thought to be phosphorylated.[1] Protein phosphorylation is one of the major known signal transduction mechanisms for controlling and regulating intercellular processes.[2] Phosphorylation also alters protein activity, subcellular location, degradation, and interactions with other proteins.[3] Phosphorylation predominantly occurs on serine, threonine, or tyrosine, through the formation of a phosphoester linkage between the amino acid and the phosphate group at the side-chain hydroxyl oxygen. However, it has also been shown on histidine, lysine, and arginine through phosphoamidate bonds and on aspartic acid and glutamic acid through anhydride linkages.[4,5]

Infrared multiphoton dissociation[6−8] (IRMPD) is a fragmentation technique typically using a CO_2 laser. The sequential absorption of 10.6 μm photons increases the internal energy of ions (0.117 eV per photon) until dissociation occurs. IRMPD is a slow heating method leading to similar fragmentation to collision-induced dissociation (CID) for peptides and proteins. For these species, fragmentation occurs via a low energy proton rearrangement leading to destabilization and cleavage of an amide bond.[9,10] Additionally, labile post translational modifications (PTMs) can also be cleaved. In nonphosphorylated peptides, the IR photons are broadly absorbed, particularly into NH and OH bonds, but rapidly redistributes via vibrational coupling. The infrared (IR) radiation is resonant with one or more phosphate vibrational modes,[11,12] and therefore, with IRMPD, phosphopeptides fragment at a much lower threshold than their unphosphorylated counterpart, in both negative[13,14] and in positive[15,16] ionization modes.

Phosphates are considered labile groups in mass spectrometry and produce diagnostic ions under CID or IRMPD fragmentation. Depending on the charge state of the peptide and the amino acid the phosphate is linked to, the fragmentation pathway is different[17,18] and leads to the loss of phosphoric acid (H_3PO_4) or metaphosphoric acid (HPO_3) in positive mode and phosphite (PO_3) in negative mode. Phosphorylated peptides are selectively detected in complex mixtures by diagnostic ions[19,20] or neutral loss from the precursor.[21,22] Radical-mediated techniques such as ECD and ETD fragment selectively at the peptide backbone and, therefore, allow the sequencing of the phosphopeptide without the loss of the phosphate group allowing localization.[23,24]

Usually complex samples are analyzed by liquid chromatography−tandem mass spectrometry (LC−MS/MS), the compounds are separated by liquid chromatography and then fragmented and detected in the mass analyzer. Two-dimensional mass spectrometry (2DMS) is an alternative technique that enables the direct infusion of the sample, without the need

Received: February 27, 2020
Accepted: April 14, 2020
Published: April 14, 2020

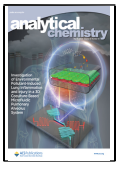

https://dx.doi.org/10.1021/acs.analchem.0c00884
Anal. Chem. 2020, 92, 6817−6821

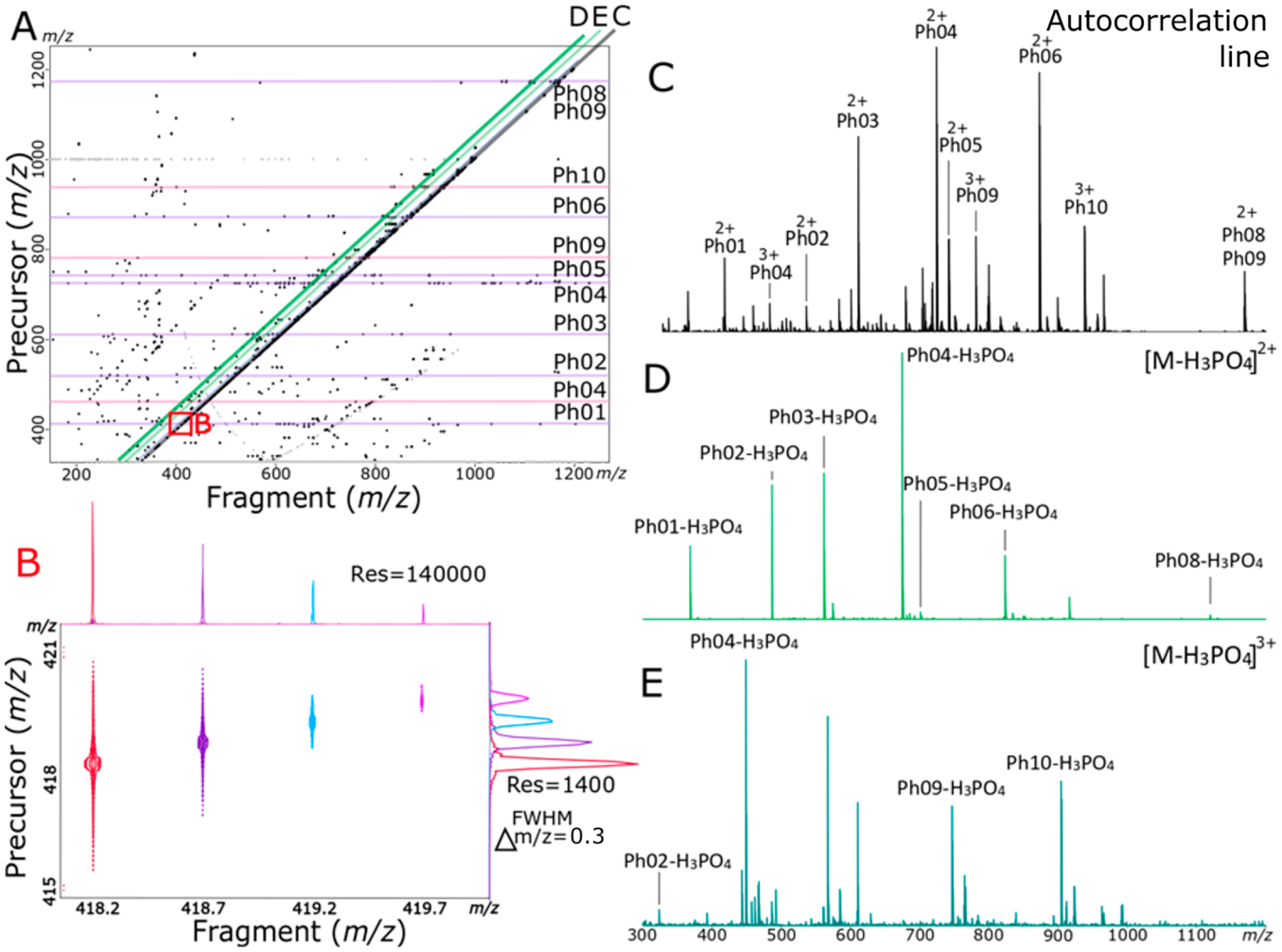

Figure 1. (A) Full 2DMS spectrum of phosphopeptide mixture; color code in Figure 1A: purple, 2+ species; pink, 3+ species. (B) Zoom of $[Ph01 + 2H]^{2+}$. Resolution in the vertical and the horizontal axes. (C) Autocorrelation line reveals all the fragmented precursors (similar to a 1D MS spectrum). (D) Extracted 2+ phosphate neutral (H_3PO_4) loss line. (E) Extracted 3+ phosphate neutral (H_3PO_4) loss line.

for liquid chromatography separation or quadrupole isolation of the species and retains the information on which fragment ions are formed from which precursors.

In a Fourier transform-ion cyclotron resonance (FT-ICR) instrument,[25,26] 2DMS uses a nonstandard pulse sequence.[27,28] Before excite/detect, ions are modulated radially in the ICR cell before the in-cell fragmentation event, using a first excitation, then delay, followed by a second excitation sequence. The pulse sequence separates ions in space depending of their m/z. Spatially resolved in-cell fragmentation methods such as IRMPD, ultraviolet photodissociation (UVPD), or electron activated dissociation (ExD) may be used for 2DMS. Scans are accumulated with an incremental delay, thereby the ions modulates in and out of the central fragmentation zone of the cell over successive scans. In each scan, the ions are at a different radius in the ICR cell and undergo different extents of fragmentation. The modulation of intensities of the precursor and its fragments with each scan is the same but opposite phase. Computing the intensities permits the creation of a 2DMS spectrum where all the fragments are correlated to their precursors. The 2DMS spectrum is a three-dimensional plot of precursor m/z, fragment m/z, and intensity, usually shown as a contour plot.[29] Figure 1b shows the projections of the actual 3-dimensional peakshape along the top and sides, and clearly demonstrates that, because of the Fourier transform, 2DMS provides full peakshapes in both dimensions which means that peak centroids in each dimension are more accurate than the full peak width.

The 2DMS sequence pulse has been previously optimized for IRMPD.[30] IRMPD 2DMS was carried out in the analysis of Angiotensin I,[31] cytochrome C,[32] and calmodulin,[33] but also in the analysis of polymers.[34] To date, for post-translational modification, only glycosylation has been analyzed by 2DMS.[35]

One of the limitations of phosphoproteomics is the phosphopeptide loss because of its increase hydrophilicity during the sample preparation or subsequent liquid chromatography in reverse phase column. In the 2DMS workflow, the direct infusion strategy allows avoidance of these losses. The nanoelectrospray ion source[36] also allows the detection of low concentration phosphopeptides.[37] The extraction of neutral loss lines in 2DMS selectively identifies phosphopeptides.

METHODS

MS Phosphomix 1 Light was obtained from Sigma (MSP1L-1VL) and contained 10 phosphopeptides: Ph01, VLHSGpSR; Ph02, RSpYpSRSR; Ph03, RDSLGpTYSSR; Ph04, pTKLIpTQLRDAK; Ph05, EVQAEQPSSpSSPR; Ph06,

https://dx.doi.org/10.1021/acs.analchem.0c00884
Anal. Chem. 2020, 92, 6817−6821

ADEPpSSEESDLEIDK; Ph07, ADEPSpSEEpSDLEIDK; Ph08, FEDEGAGFEESpSETGDYEEK; Ph09, ELSNpSPLRENSFGpSPLEFR; and Ph10, SPTEYHEPVpYANPFYRPTpTPQR. Water was purified by a Millipore Direct-Q purification system (Merck Millipore, MA). Acetonitrile was obtained from VWR Chemicals (CAS, 75-05-8). Formic acid was obtained from Sigma-Aldrich (CAS, 64-18-6).

Phosphomix (30 μL, 80:20 water−ACN + 0.1% FA, 0.2 μM) was ionized using a custom nanoelectrospray ionization source (nESI) using a pulled glass capillary with several micrometers open orifice. Mass spectrometry was conducted using a 12 T Bruker solariX FTICR mass spectrometer (Bruker Daltonik GmbH, Bremen, Germany), and IRMPD fragmentation was achieved using a continuous wave, 25 W, CO_2 laser (Synrad Inc., Washington) for 0.135 s at a laser power of 40%. A total of 8192 scans of 1 M (16-bit) data points were acquired over a mass range of m/z 328−3000 on the vertical (precursor) axis and m/z 147−3000 on the horizontal (fragment) axis. The 2DMS experiment was acquired over 170 min. (1.25 s per scan). The data was processed with SPIKE,[38] using urQRd[39] with rank 15. Spectra were extracted using T2D[40] and they were internally calibrated using known fragment peaks with a quadratic calibration function in the Bruker DataAnalysis v4.3 software (Bruker Daltonics GmbH, Bremen, Germany).

RESULTS AND DISCUSSION

All phosphopeptides were analyzed simultaneously without prior liquid chromatography separation or quadrupole isolation. Figure 1A shows the complete 2D spectrum as a contour plot. The autocorrelation line (Figure 1C), extracted for the diagonal line of Figure 1A with $x = y$, reveals all of the fragmented precursors and is similar to a standard MS scan.

Horizontal lines are fragment ion scan lines (Figure 2B), discussed below, and correlate the fragments of a given precursor. Any horizontal line may be extracted and analyzed in Bruker's DataAnalysis software using an in-house generated T2D software, which rewrites the 2DMS scan lines into a format that DataAnalysis can read.

In Figure 1B, the phosphopeptide Ph01 is shown at charge state 2+. The resolution in the horizontal dimension is around 140 000 at m/z 420, which is consistent with a 0.4194 s transient (1 MW) at 12 T. The resolution in the vertical axis is around 1400 at m/z 420, which is consistent with the collection of the 8192 data points (scans) in the second dimension.

Figure 1D,E is extracted neutral loss lines and corresponds to a loss of 49 and 32.5 Da which corresponds to the loss of H_3PO_4 (98 Da) in 2+ and 3+ charge states, respectively. The extraction of the neutral loss lines quickly reveals the phosphopeptides in the mixture.

Nine of the ten phosphopeptides in the mixture were found in the extracted phosphate loss lines. The case of Ph07, which was not found, will be discussed below. Other phosphopeptides were detected, and they are expected to be synthetic byproducts. No phosphate migration was detected. The focus will be on the 10 major compounds. For each detected precursor, it is possible to extract a horizontal line containing the fragments of that precursor. Table 1 contains all the information on the phosphopeptides extracted from the 2DMS spectra with cleavages marked and the region of the phosphate localization highlighted. In most of the phosphopeptides, no fragments with the loss of the phosphate group was detected along with the fragment containing the phosphate. Therefore, the localization of the phosphate group was assigned using all fragments.

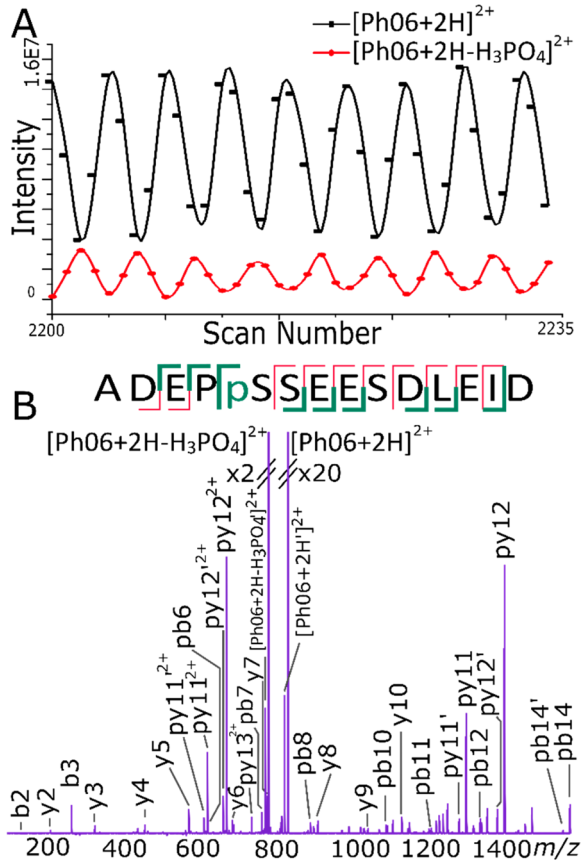

Figure 2. Example of phosphopeptide Ph06. (A) Modulation of intensities of the precursor Ph06 in black and in red the fragment of Ph06 corresponding to the loss of phosphate (B-spline). (B) Extracted fragment line of Ph06, loss of water; p, fragment with a phosphate group attached. In the cleavage diagram: green, bold, b/y fragment with a phosphate group; red, b/y fragment without a phosphate group.

The IRMPD pulse length was optimized beforehand in a 1DMS experiment for the fragmentation of medium sized phosphopeptides. Ph06 was quadrupole isolated and fragmented at different IRMPD pulse lengths. A 0.135 s IRMPD pulse length gave the best cleavage coverage for the peptide and was selected for the analysis of the complex mixture.

Therefore, Ph03, Ph04, Ph05, Ph06, and Ph08 have high cleavage coverage (∼75%). The smaller peptide Ph01 and Ph02 are over fragmented. The phosphate group on the tyrosine on Ph02 is cleaved in the fragments b3, pb4, and pb5. Therefore, the localization of the phosphate group on the tyrosine is lost; the localization of the phosphate group on serine is retained for Ph02. Ph09 and Ph10 showed lower cleavage coverage (∼25%) due to their longer length. The site of the phosphate was determined in 11 out of the 13 phosphorylation sites.

During the 2DMS pulse sequence, ions are separated radially before fragmentation. For each scan, the precursor is at a different radius at the time of fragmentation. Therefore, the precursor ion intensity oscillates over the various scans depending on its own cyclotron frequency and magnitude of fragmentation.

https://dx.doi.org/10.1021/acs.analchem.0c00884
Anal. Chem. 2020, 92, 6817−6821

Table 1. Observed Cleavage Coverage of the Detected Phosphopeptides by 2DMS[a]

	Cleavage Coverage
Ph01	VLHSGpSR
Ph02	RSpYpSRSR
Ph03	RDSLGpTYSSR
Ph04	pTKLIpTQLRDAK
Ph05	EVQAEQPSSpSSPR
Ph06	ADEPpSSEESDLEID
Ph08	FEDEGAGFEESpSETGDYEEK
Ph09	ELSNpSPLRENSFGpSPLEFR
Ph10	SPTEYHEPVpYANPFYRPTpTPQ

[a]Green, bold, b/y fragment containing a single phosphate; green, double lined, b/y fragment containing two phosphates; red, b/y fragment without a phosphate group; green box, localization of the phosphate group.

With phosphopeptides, using IRMPD, the most intense fragment is usually the loss of the phosphate. The intensity of the fragment ions have the same modulation frequency as of the precursor but opposite phase (Figure 2A).[41]

All observed precursors had different m/z values and therefore different cyclotron frequencies in the ion cyclotron cell. The frequency of modulation of the intensities over the scan enables the differentiation of which fragments are derived from which precursors in a complex mixture.

The intensity of the phosphate loss fragment of Ph05 is low (Figure 1D). Low-intensity phosphate loss fragments have been seen in the literature when the phosphopeptide undergoes a different fragmentation pathway, especially with phosphothreonine and phosphotyrosine containing peptides.[16] However, the phosphate on Ph05 was localized to the serine, so an alternate mechanism was not expected. Ph05 has few amino acids (arginine, serine, and glutamic acid) with the potential of having hydrogen bonds with the phosphate group, which could lead to a stabilization of the phosphorylation and explain why there are less phosphate loss fragments.

The 2DMS experiment enables the simultaneous fragmentation of all the phosphopeptides without prior separation or isolation; the data collected shows no indication of different behavior between the peptides with serine, threonine, or tyrosine phosphorylation.

Ph07 was not detected in the neutral phosphate loss lines and at very low intensity in the autocorrelation line. After further investigation (Figure S2), it has been found that Ph07 was only detected for a brief amount of time in a chromatography mode experiment. The loss of Ph07 was, therefore, not due to the 2DMS experiment. Ph07 is a very hydrophobic peptide; it undergoes adsorption at the glass surface of the pulled glass capillary used in the direct infusion experiment.

CONCLUSION

Two-dimensional mass spectrometry enabled the characterization of a mixture of phosphopeptides. The extraction of neutral loss lines enabled their selective identification. In total, 90% of the phosphopeptides were assigned in a single direct infusion experiment without the need for liquid chromatography separation or quadrupole isolation. High cleavage coverage was achieved, and the localization of the phosphate was not lost during the fragmentation.

The obtained resolving power was sufficient for confident assignment of the precursors and the fragments in this experiment. However, to increase the resolution of the 2DMS spectra, it is possible to acquire a longer transient for each scan to increase the horizontal resolution power or to increase the number of scans to increase the vertical resolving power. In both cases, more acquisition time and more processing time are required due to the size of the resulting data file.

To investigate a full phosphoproteome, the 2DMS experiment could be done on wide m/z quadrupole isolated windows. Each of the windows would have their own optimized IRMPD pulse length, depending of the size of the precursors in the mass-to-charge ratio window. The method presented shows a data independent approach for phosphopeptide analysis and fragmentation analysis independent of liquid chromatography.

ASSOCIATED CONTENT

Supporting Information

The Supporting Information is available free of charge at https://pubs.acs.org/doi/10.1021/acs.analchem.0c00884.

Precurors, comparison between 1D standard MS scan and extracted 2DMS autocorrelation line, tables of assignments for all the spectra, and cleavage coverage map (PDF)

AUTHOR INFORMATION

Corresponding Author

Peter B. O'Connor − *University of Warwick, Department of Chemistry, Coventry CV4 7AL, United Kingdom;* orcid.org/0000-0002-6588-6274; Phone: +44 (0) 2476 151 008; Email: p.oconnor@warwick.ac.uk

Authors

Johanna Paris − *University of Warwick, Department of Chemistry, Coventry CV4 7AL, United Kingdom*

Tomos E. Morgan − *University of Warwick, Department of Chemistry, Coventry CV4 7AL, United Kingdom;* orcid.org/0000-0002-3366-8889

Christopher A. Wootton − *University of Warwick, Department of Chemistry, Coventry CV4 7AL, United Kingdom;* orcid.org/0000-0002-3647-2611

Mark P. Barrow − *University of Warwick, Department of Chemistry, Coventry CV4 7AL, United Kingdom;* orcid.org/0000-0002-6474-5357

John O'Hara − *UCB, Slough SL1 3WE, United Kingdom*

Complete contact information is available at: https://pubs.acs.org/10.1021/acs.analchem.0c00884

Author Contributions

The manuscript was written through contributions of all authors.

https://dx.doi.org/10.1021/acs.analchem.0c00884
Anal. Chem. 2020, 92, 6817−6821

Notes

The authors declare no competing financial interest.

■ ACKNOWLEDGMENTS

The authors would like to thank Bryan Marzullo, Yuko Lam, and Maria van Agthoven for their help as well as all the ICR lab for their support. Johanna Paris thanks EPSRC for a Ph.D. studentship through the EPSRC Centre for Doctoral Training in Molecular Analytical Science, Grant Number EP/L015307/1, UCB, BB/R022399/1, BB/P021879/1, EP/N033191/1, and Horizon 2020 EU FTICR MS network (Grant 731077) for funding.

■ REFERENCES

(1) Cohen, P. *Nat. Cell Biol.* **2002**, *4*, E127−E130.
(2) Pawson, T.; Scott, J. D. *Trends Biochem. Sci.* **2005**, *30*, 286−290.
(3) Cohen, P. *Trends Biochem. Sci.* **2000**, *25*, 596−601.
(4) Cieśla, J.; Frączyk, T.; Rode, W. *Acta Biochim. Polym.* **2011**, *58*, 137−148.
(5) Hardman, G.; Perkins, S.; Ruan, Z.; Kannan, N.; Brownridge, P.; Byrne, D. P.; Eyers, P. A.; Jones, A. R.; Eyers, C. E. *bioRxiv* **2017**, 202820.
(6) Little, D. P.; Speir, J. P.; Senko, M. W.; O'Connor, P. B.; McLafferty, F. W. *Anal. Chem.* **1994**, *66*, 2809−2815.
(7) Talebpour, A.; Bandrauk, A.; Yang, J.; Chin, S. *Chem. Phys. Lett.* **1999**, *313*, 789−794.
(8) Maitre, P.; Scuderi, D.; Corinti, D.; Chiavarino, B.; Crestoni, M. E.; Fornarini, S. J. C. R. *Chem. Rev.* **2019**, *120*, 3261−3295.
(9) McCormack, A. L.; Somogyi, A.; Dongre, A. R.; Wysocki, V. H. *Anal. Chem.* **1993**, *65*, 2859−2872.
(10) Tsaprailis, G.; Nair, H.; Somogyi, Á.; Wysocki, V. H.; Zhong, W.; Futrell, J. H.; Summerfield, S. G.; Gaskell, S. J. *J. Am. Chem. Soc.* **1999**, *121*, 5142−5154.
(11) Correia, C. F.; Balaj, P. O.; Scuderi, D.; Maitre, P.; Ohanessian, G. *J. Am. Chem. Soc.* **2008**, *130*, 3359−3370.
(12) Stedwell, C. N.; Patrick, A. L.; Gulyuz, K.; Polfer, N. C. *Anal. Chem.* **2012**, *84*, 9907−9912.
(13) Flora, J. W.; Muddiman, D. C. *J. Am. Chem. Soc.* **2002**, *124*, 6546−6547.
(14) Flora, J. W.; Muddiman, D. C. *J. Am. Soc. Mass Spectrom.* **2004**, *15*, 121−127.
(15) Crowe, M. C.; Brodbelt, J. S. *J. Am. Soc. Mass Spectrom.* **2004**, *15*, 1581−1592.
(16) Crowe, M. C.; Brodbelt, J. S. *Anal. Chem.* **2005**, *77*, 5726−5734.
(17) DeGnore, J. P.; Qin, J. *J. Am. Soc. Mass Spectrom.* **1998**, *9*, 1175−1188.
(18) Rožman, M. *J. Mass Spectrom.* **2011**, *46*, 949−955.
(19) Huddleston, M. J.; Annan, R. S.; Bean, M. F.; Carr, S. A. *J. Am. Soc. Mass Spectrom.* **1993**, *4*, 710−717.
(20) Flora, J. W.; Muddiman, D. C. *Anal. Chem.* **2001**, *73*, 3305−3311.
(21) Carr, S. A.; Huddleston, M. J.; Annan, R. S. *Anal. Biochem.* **1996**, *239*, 180−192.
(22) Chang, E. J.; Archambault, V.; McLachlin, D. T.; Krutchinsky, A. N.; Chait, B. T. *Anal. Chem.* **2004**, *76*, 4472−4483.
(23) Stensballe, A.; Jensen, O. N.; Olsen, J. V.; Haselmann, K. F.; Zubarev, R. A. *Rapid Commun. Mass Spectrom.* **2000**, *14*, 1793−1800.
(24) Song, H.; Håkansson, K. *Anal. Chem.* **2012**, *84*, 871−876.
(25) Amster, I. J. *J. Mass Spectrom.* **1996**, *31*, 1325−1337.
(26) Marshall, A. G.; Hendrickson, C. L.; Jackson, G. S. *Mass Spectrom. Rev.* **1998**, *17*, 1−35.
(27) Pfändler, P.; Bodenhausen, G.; Rapin, J.; Houriet, R.; Gäumann, T. *Chem. Phys. Lett.* **1987**, *138*, 195−200.
(28) Pfändler, P.; Bodenhausen, G.; Rapin, J.; Walser, M. E.; Gaeumann, T. *J. Am. Chem. Soc.* **1988**, *110*, 5625−5628.
(29) van Agthoven, M. A.; Lam, Y. P.; O'Connor, P. B.; Rolando, C.; Delsuc, M.-A. *Eur. Biophys. J.* **2019**, *48*, 213−229.
(30) van Agthoven, M. A.; Chiron, L.; Coutouly, M.-A.; Sehgal, A. A.; Pelupessy, P.; Delsuc, M.-A.; Rolando, C. *Int. J. Mass Spectrom.* **2014**, *370*, 114−124.
(31) van Agthoven, M. A.; Delsuc, M.-A.; Rolando, C. *Int. J. Mass Spectrom.* **2011**, *306*, 196−203.
(32) van Agthoven, M. A.; Wootton, C. A.; Chiron, L.; Coutouly, M.-A.; Soulby, A.; Wei, J.; Barrow, M. P.; Delsuc, M.-A.; Rolando, C.; O'Connor, P. B. *Anal. Chem.* **2016**, *88*, 4409−4417.
(33) Floris, F.; van Agthoven, M.; Chiron, L.; Soulby, A. J.; Wootton, C. A.; Lam, Y. P.; Barrow, M. P.; Delsuc, M.-A.; O'Connor, P. B. *J. Am. Soc. Mass Spectrom.* **2016**, *27*, 1531−1538.
(34) Floris, F.; Vallotto, C.; Chiron, L.; Lynch, A. M.; Barrow, M. P.; Delsuc, M.-A.; O'Connor, P. B. *Anal. Chem.* **2017**, *89*, 9892−9899.
(35) van Agthoven, M. A.; Chiron, L.; Coutouly, M.-A.; Delsuc, M.-A.; Rolando, C. *Anal. Chem.* **2012**, *84*, 5589−5595.
(36) Wilm, M.; Mann, M. *Anal. Chem.* **1996**, *68*, 1−8.
(37) Wilm, M.; Neubauer, G.; Mann, M. *Anal. Chem.* **1996**, *68*, 527−533.
(38) Chiron, L.; Coutouly, M.-A.; Starck, J.-P.; Rolando, C.; Delsuc, M.-A. SPIKE a Processing Software dedicated to Fourier Spectroscopies. *arXiv*, **2016**, 1608.06777
(39) Chiron, L.; van Agthoven, M. A.; Kieffer, B.; Rolando, C.; Delsuc, M.-A. *Proc. Natl. Acad. Sci. U. S. A.* **2014**, *111*, 1385−1390.
(40) Wootton, C. A.; Morgan, T. E.; Marzullo, B. P.; Lam, Y. P. Y.; Lozano, D. C. P.; Theisen, A.; Haris, A.; Barrow, M. P.; O'Connor, P. B. Ultra-high resolution 2D-FTMS for truly DIA analysis of challenging systems. In *Proceedings of the 67th ASMS Conference on Mass Spectrometry and Allied Topics*, Atlanta, GA, June 2−6, 2019; 298156.
(41) van Agthoven, M. A.; Kilgour, D. P.; Lynch, A. M.; Barrow, M. P.; Morgan, T. E.; Wootton, C. A.; Chiron, L.; Delsuc, M.-A.; O'Connor, P. B. *J. Am. Soc. Mass. Spectrom.* **2019**, *30*, 2594−2607.

https://dx.doi.org/10.1021/acs.analchem.0c00884
Anal. Chem. 2020, 92, 6817−6821